Title: The emergence of heat and humidity too severe for human tolerance

Authors: Colin Raymond[1]*, Tom Matthews[2], and Radley M. Horton[1,3]

Affiliations:
[1]Department of Earth and Environmental Sciences, Columbia University, New York, NY, USA.
[2]Department of Geography and Environment, Loughborough University, Loughborough, UK.
[3]Lamont-Doherty Earth Observatory, Columbia University, Palisades, NY, USA.

*Corresponding author. Email: cr2630@columbia.edu

One Sentence Summary: Extreme humid heat is closer to humans' physiological limit than previously reported, and the margin is being cut more rapidly than models project.

Abstract:

Humans' ability to efficiently shed heat has enabled us to range over every continent, but a wet-bulb temperature of 35°C marks our upper physiological limit, and severe health and productivity impacts occur at lower values. Climate models first project 35°C occurrences only late this century under high-end emissions scenarios. Conducting a comprehensive observational evaluation, we show the first evidence that some subtropical locations have already reached 35°C, and that occurrences of extreme humid heat overall have more than doubled since 1979. Our results shift earlier by decades the projected period when global-maximum TW values regularly exceed 35°C. We also discover strong relationships with sea-surface temperatures, which are themselves approaching dangerously high values. Our findings underscore the exceptional challenge posed to society by extreme humid heat.

Main Text:

Humans' bipedal locomotion, naked skin, and sweat glands are constituents of a sophisticated cooling system *(1)*. Despite these thermoregulatory adaptations, extreme heat remains one of our most dangerous natural hazards *(2)*, with tens of thousands of fatalities in the deadliest events so far this century *(3,4)*. The combined impacts of heat and humidity are well-established and extend beyond direct health outcomes to include reduced individual performance

across a range of activities, as well as larger-scale economic impacts *(5-7)*. Heat-humidity impacts have prompted decades of study in military, athletic, and occupational contexts *(8,9)*. However, consideration of TW from a climate perspective only began more recently *(10,11)*.

While some heat-humidity impacts can be avoided through acclimation and behavioral adaptation *(12)*, there exists a hard upper limit for survivability, even under idealized conditions of perfect health, total inactivity, full shade, absence of clothing, and unlimited drinking water *(9,10)*. Our normal internal body temperature of 36.8 ± 0.5°C requires skin temperatures of around 35°C to maintain a gradient directing heat outward from the core *(10,13)*. Once the air (dry-bulb) temperature rises above this threshold, metabolic heat can only be shed via sweat-based latent cooling, and at TW exceeding 35°C, this cooling mechanism loses its effectiveness altogether. Because the ideal assumptions are almost never met, severe impacts occur at much lower values — for example, most regions affected by the deadly 2003 European and 2010 Russian heatwaves experienced TW no greater than 28°C (Fig. S1). In the literature to date, there have been no observational reports of TW exceeding 35°C, and few reports exceeding 33°C *(9,11,14,15)*. The awareness of a physiological limit has prompted modeling studies to ask how soon it may be crossed. Results suggest that, under a business-as-usual RCP8.5 warming scenario, TW could exceed 35°C in South Asia and the Middle East by the end of the century *(14-16)*.

Here, we use quality-assured station observations *(17,18)* and high-resolution reanalysis data *(19,20)* to establish the baseline values and geographic patterns of TW, and to use recent trends in TW and in SSTs to provide observationally based constraints on future TW projections as climate change continues.

In contrast to these earlier studies, we find large numbers of TW exceedances of 31°C and 33°C, and that three stations in the dataset have recorded multiple daily-maximum TW values

already exceeding 35°C. These are exceptional conditions, beyond prolonged human tolerance. The three aforementioned stations are Dhahran/Dammam (Saudi Arabia, population 1.1 million); Doha (Qatar, population 1.75 million); and Ras Al Khaimah (UAE, population 0.3 million), all located on the southern Persian Gulf, which is known to reach extraordinarily high SSTs in late spring and summer and consequently favor the occurrence of extreme humid heat *(2,14)*. These conclusions are supported by regionally coherent observational evidence: of the stations in the Persian Gulf area with at least 90% data availability, all have a historical 99.9th percentile of TW (the value exceeded roughly 14 times in the 39 years studied) above 31°C (Fig. 1; see Fig. S1 for the all-time maximum observed TW). In ERA-Interim, the highest values are also confined to the southern fringe of the Persian Gulf (Fig. S2). Its global highest TW has come very close to, but not yet reached, the 35°C threshold (Fig. 2).

Other >31°C hotspots emerge through the 99.9th percentile metric: eastern coastal India, northwestern India, Pakistan, northwestern Australia, and the shores of the Red Sea, Gulf of California, and Gulf of Mexico (Fig. 1). All are situated in the subtropics, along coastlines (often with a semi-enclosed gulf or bay of shallow depth, limiting ocean circulation and facilitating high SSTs), and in proximity to sources of continental heat, which along with the maritime air seem to be the necessary ingredients for truly extraordinary TW values to occur *(11)*. The exception to the coastline rule is western South Asia, perhaps due to the efficient inland transport of humid air by the summer monsoon in combination with large-scale irrigation *(15,21)*. Tropical-forest and maritime areas generally experience TW no higher than 31-32°C, likely because of the high evapotranspiration potential and cloud cover, along with the greater instability of the tropical atmosphere. However, more research is needed on the thermodynamic mechanisms that prevent these areas from reaching higher values.

Steep and statistically significant upward trends in extreme TW frequency (exceedances of 27°C, 29°C, and 31°C) and magnitude are present in HadISD and ERA-Interim, coincident with the rise in global-mean air temperature (Fig. 2). Each of the frequency trends represents more than a doubling of occurrences of the corresponding threshold between 1979 and 2017. We also find a sharp peak in the number of global TW extremes for many thresholds during the strong El Niño events of 1998 and 2016. Detrending reveals that this El Niño-Southern Oscillation [ENSO] correlation is largest for TW values that are high but not exceptional across the tropics and subtropics – for instance, 27°C and 29°C (Fig. S3). This phenomenon may be related to the effect of ENSO on hydrological extremes at the global scale, on tropospheric-mean temperatures, or on SSTs in particular basins, but further work is necessary to test these new hypotheses *(22,23)*. At the regional scale, we find that for the hotspot basins of the Bay of Bengal and the Gulf of Mexico, summer average SSTs correlate well ($r>0.7$) on a detrended interannual basis with the count of extreme-TW occurrences on the surrounding coasts. This modulation of extreme TW by SSTs is consistent with previous assessments along the United States coast *(24)*.

Modulation is also seen in the seasonal cycle of TW extremes. As a joint function of temperature and humidity, TW has a seasonal cycle in its extremes distinct from that of temperature alone, and this is seen most clearly in monsoonal regions. For South Asia, the timing of peak TW varies with the advance of the summer monsoon *(15)*. Splitting South Asia into 'early monsoon' and 'late monsoon' subregions, we find that the number of TW extremes is largest just prior to the local climatological monsoon onset date (Fig. S4). While equivalent extreme values of TW are possible before, during, and after the monsoon rains in any given year, they are of a different character: low relative humidity before the monsoon starts, and then

become progressively moister as summer progresses. This result emphasizes the variations in the circumstances that can lead to extreme humid heat even in the same location, and suggests that impacts-mitigation strategies may benefit from taking this distinction into account.

The aforementioned significant correlation between annual TW maxima and global-mean air temperature (series plotted in the bottom two panels of Figure 2; r=0.53; p=0.001) enables fitting a non-stationary generalized extreme value [GEV] distribution to model the 30-year return value for global maximum TW as a function of global-warming amount. Relative to pre-industrial, 30-year maximum TW at the ERA-I resolution has increased by almost 1°C. By the time global warming reaches 1.9°C, our GEV projection's central estimate suggests that the 30-year global return value will exceed the 35°C limit (Fig. 3). These observationally-constrained analyses therefore suggest relatively large-scale exceedances of this critical value should be expected between the Paris targets of 1.5°C and 2°C of global warming.

To assess the physical realism of our GEV extrapolation, we also examine independent maximum monthly SSTs. An atmospheric boundary layer fully equilibrated with the ocean surface would be at saturation and have the same temperature as the underlying SSTs, meaning that in principle 35°C is the lowest SST that could sustain the critical 35°C value of TW in the air above. In reality, equilibrium will not be achieved if air-mass residence times over extreme SSTs are too short, which may be more likely if strong surface heating triggers deep convection *(10)*. Current SSTs provide some guidance as to whether projections of TW above 35°C are physically plausible in marine and coastal environments. In this context, we find that SSTs have already exceeded 35°C in the Persian Gulf, reaching 35.2°C in 2017 (Fig. S5). The extraordinary 2017 SSTs are, however, an outlier to the preceding timeseries, so we exploit the correlation between SSTs and global-mean temperature to investigate the amount of climate warming required before such exceedances could

be the norm. The results provide physically based support to the GEV analysis, predicting maximum monthly-mean SSTs will routinely reach 35°C for about 2.1°C of warming from pre-industrial (1.5-3.0°C; 95% confidence interval) (Fig. 3).

Our findings indicate that occurrences of extreme TW have increased rapidly at weather stations and in reanalysis data over the last four decades, and that parts of the planet are very close to the 35°C survivability limit, which may have already been reached near the shores of the Persian Gulf. The trends we describe indicate with new clarity that, for significant areas of the world, the buffer between current observations and 35°C has been reduced considerably by the global warming to date. TW exceeding 35°C has not yet been realized at the larger spatial scale of reanalysis data, but according to our assessment, this is possible with around 2°C of warming since pre-industrial, rather than requiring more severe warming scenarios as postulated in prior work *(10,14-16)*.

Taken together, our work underlines that the planet is in the process of transitioning to a climate state featuring extremes well outside the range of past natural variability in which our physiology evolved *(25)*. Beyond 2°C of global warming from pre-industrial, this transition will be largely complete *(26)*. The deadly heat events already experienced in recent decades are indicative of the growing societal challenges resulting from extreme humid heat.

References and Notes:

1. P. E. Wheeler, The thermoregulatory advantages of hominid bipedalism in open equatorial environments: the contribution of increased convective heat loss and cutaneous evaporative cooling. *J. Hum. Evol.* **21,** 107–115 (1991). doi:10.1016/0047-2484(91)90002-D

2. M. Wehner, D. Stone, H. Krishnan, K. AchutaRao, F. Castillo, The deadly combination of heat and humidity in India and Pakistan in summer 2015. In "Explaining Extreme Events of 2015 from a Climate Perspective" [S. C. Herring, A. Hoell, M. P. Hoerling, J. P. Kossin, C. J. Schreck III, P. A. Stott, P. A., Eds.]. *Bull. Amer. Meteorol. Soc.,* **97** (12), Suppl. (2016). doi:10.1175/bams-d-16-0145.1

3. J.-M. Robine, S. L. K. Cheung, S. Le Roy, H. Van Oyen, C. Griffiths, J.-P. Michel, F. R. Herrmann, Death toll exceeded 70,000 in Europe during the summer of 2003. *C. R. Biol.* **331,** 171–178 (2008). doi:10.1016/j.crvi.2007.12.001

4. B. A. Revich, Heat-wave, air quality and mortality in European Russia in summer 2010: preliminary assessment. Ekol. Cheloveka Hum. Ecol. 3–9 (2011).

5. T. K. R. Matthews, R. L. Wilby, C. Murphy, Communicating the deadly consequences of global warming for human heat stress. *Proc. Nat. Acad. Sci.* **114,** 3861–3866 (2017). doi:10.1073/pnas.1617526114

6. C. Mora, B. Dousset, I. R. Caldwell, F. E. Powell, R. C. Geronimo, C. R. Bielecki, C. W. B. S. Dietrich, E. T. Johnston, L. V. Louis, M. P. Lucas, M. M. McKenzie, A. G. Shea, H. Tseng, T. W. Giambelluca, L. R. Leon, E. Hawkins, C. Trauernicht, Global risk of deadly heat. *Nat. Clim. Change* **7,** 501–506 (2017). doi:10.1038/nclimate3322

7. T. Kjellstrom, D. Briggs, C. Freyberg, B. Lemke, M. Otto, O. Hyatt, Heat, human performance, and occupational health: A key issue for the assessment of global climate change impacts. *Annu. Rev. Public Health,* **37,** 97-112 (2016). doi:10.1146/annurev-publhealth-032315-021740

8. M. N. Sawka, C. B. Wenger, S. J. Montain, M. A. Kolka, B. Bettencourt, S. Flinn, J. Gardner, W. T. Matthew, M. Lovell, C. Scott, Heat stress control and heat casualty management. *US Army Research Institute of Environmental Medicine Technical Bulletin 507* (2003).

9. K. Parsons, Heat stress standard ISO 7243 and its global application. *Indust. Health,* **44,** 368-379 (2006). doi:10.2486/indhealth.44.368

10. S. C. Sherwood, M. Huber, An adaptability limit to climate change due to heat stress. *Proc. Nat. Acad. Sci.* **107,** 9552–9555 (2010). doi:10.1073/pnas.0913352107

11. C. Schär, Climate extremes: The worst heat waves to come. *Nat. Clim. Change* **6,** 128–129 (2016). doi:10.1038/nclimate2864

12. D. Lowe, K. L. Ebi, B. Forsberg, Heatwave early warning systems and adaptation advice to reduce human health consequences of heatwaves. *Int. J. Environ. Res. Public. Health* **8,** 4623–4648 (2011). doi:10.3390/ijerph8124623

13. E. G. Hanna, P. W. Tait, Limitations to thermoregulation and acclimatization challenge human adaptation to global warming. *Int. J. Environ. Res. Public. Health* **12,** 8034–8074 (2015). doi:10.3390/ijerph120708034

14. J. S. Pal, E. A. B. Eltahir, Future temperature in southwest Asia projected to exceed a threshold for human adaptability. *Nat. Clim. Change* **6,** 197–200 (2016). doi:10.1038/nclimate2833

15. E.-S. Im, J. S. Pal, E. A. B. Eltahir, Deadly heat waves projected in the densely populated agricultural regions of South Asia. *Sci. Adv.* **3,** e1603322 (2017). doi:10.1126/sciadv.1603322

16. E. Coffel, R. M. Horton, A. de Sherbinin, Temperature and humidity based projections of a rapid rise in global heat stress exposure during the 21st century. *Env. Res. Lett.,* **13,** 014001 (2018). doi:10.1088/1748-9326/aaa00e

17. R. J. H. Dunn, K. M. Willett, D. E. Parker, L. Mitchell, Expanding HadISD: quality-controlled, sub-daily station data from 1931. *Geosci. Instrum. Method. Data Syst.,* **5,** 473-491 (2016). https://doi.org/10.5194/gi-5-473-2016

18. R. J. H. Dunn, K. M. Willett, P. W. Thorne, E. V. Woolley, I. Durre, A. Dai, D. E. Parker, R. S. Vose, HadISD: a quality-controlled global synoptic report database for selected variables at long-term stations from 1973-2011. *Clim. Past,* **8,** 1649-1679 (2012). doi:10.5194/cp-8-1649-2012

19. D. P. Dee, S. M. Uppala, A. J. Simmons, P. Berrisford, P. Poli, S. Kobayashi, U. Andrae, M. A. Balmaseda, G. Balsamo, P. Bauer, P. Bechtold, A. C. M. Beljaars, L. van de Berg, J. Bidlot, N. Bormann, C. Delsol, R. Dragani, M. Fuentes, A. J. Geer, L. Haimberger, S. B. Healy, H. Hersbach, E. V. Hólm, L. Isaksen, P. Kållberg, M. Köhler, M. Matricardi, A. P. McNally, B. M. Monge-Sanz, J.-J. Morcrette, B.-K. Park, C. Peubey, P. de Rosnay, C. Tavolato, J.-N. Thépaut, F. Vitart, The ERA-Interim reanalysis: configuration and performance of the data assimilation system. *Q. J. R. Meteorol. Soc.* **137**, 553–597 (2011). doi:10.1002/qj.828

20. N. A. Rayner, D. E. Parker, E. B. Horton, C. K. Folland, L. V. Alexander, D. P. Rowell, E. C. Kent, A. Kaplan, Global analyses of sea surface temperature, sea ice, and night marine air temperature since the late nineteenth century. *J. Geophys. Res. Atmos.* **108,** 4407 (2003). doi:10.1029/2002JD002670

21. T. K. R. Matthews, Humid heat and climate change. *Prog. Phys. Geog.,* **42** (3), 391-405 (2018). doi:10.1177/0309133318776490.

22. J. Sheffield, K. M. Andreadis, E. F. Wood, D. P. Lettenmaier, Global and continental drought in the second half of the twentieth century: severity-area-duration analysis and temporal variability of large-scale events. *J. Clim.,* **22,** 1962-1981 (2009). doi:10.1175/2008jcli2722.1

23. A. H. Sobel, I. M. Held, C. S. Bretherton, The ENSO signal in tropical tropospheric temperature. *J. Clim.,* **15,** 2702-2706 (2002). doi:10.1175/1520-0442(2002)015<2702:TESITT>2.0.CO;2

24. C. Raymond, D. Singh, R. M. Horton, Spatiotemporal patterns and synoptics of extreme wet-bulb temperature in the contiguous United States. *J. Geophys. Res. Atmos.,* **122** (2017). doi:10.1002/2017jd027140

25. J. Marsicek, B. N. Shuman, P. J. Bartlein, S. L. Shafer, S. Brewer, Reconciling divergent trends and millennial variations in Holocene temperatures. *Nature* **554,** 92–96 (2018). doi:10.1038/nature25464

26. C.-F. Schleussner, T. K. Lissner, E. M. Fischer, J. Wohland, M. Perrette, A. Golly, J. Rogelj, K. Childers, J. Schewe, K. Frieler, M. Mengel, W. Hare, M. Schaeffer, Differential climate impacts for policy-relevant limits to global warming: the case of 1.5°C and 2°C. *Earth Sys. Dyn*. **7,** 327–351 (2016). doi:10.5194/esd-7-327-2016

27. C. P. Morice, C. P., J. J. Kennedy, N. A. Rayner, P. D. Jones, Quantifying uncertainties in global and regional temperature change using an ensemble of observational estimates: The HadCRUT4 data set. *J. Geophys. Res. Atmos.* **117** (2012). doi:10.1029/2011JD017187

28. J. R. Buzan, K. Oleson, M. Huber, Implementation and comparison of a suite of heat stress metrics within the Community Land Model version 4.5. *Geosci. Model Dev.,* **8,** 151-170 (2015). doi:10.5194/gmd-8-151-2015

29. R. Davies-Jones, An efficient and accurate method for computing the wet-bulb temperature along pseudoadiabats. *Mon. Wea. Rev.,* **136,** 2764-2785 (2008). doi:10.1175/2007mwr2224.1

30. Demographia. Demographia World Urban Areas, 14th Edition (2018). *http://www.demographia.com/db-worldua.pdf*.

31. Ras Al Khaimah. *https://www.government.ae/en/about-the-uae/the-seven-emirates/ras-al-khaimah* (2018).

Acknowledgments: Code for computing the wet-bulb temperature using the Davies-Jones formulae was provided by Robert Kopp at Rutgers University.

Funding: Funding for R. M. H. and C. R. was provided by the National Oceanic and Atmospheric Administration's Regional Integrated Sciences and Assessments program, grant NA15OAR4310147.

Author contributions: C. R. and T. M. produced the datasets and conducted the analyses. C. R., T. M., and R. M. H. collectively developed ideas and wrote the manuscript.

Competing interests: The authors declare no competing interests.

Data and materials availability: Datasets are described in the supplementary materials. Data and code used in the analysis will be made publicly available in a Github repository at https://github.com/cr2630git/humidheat

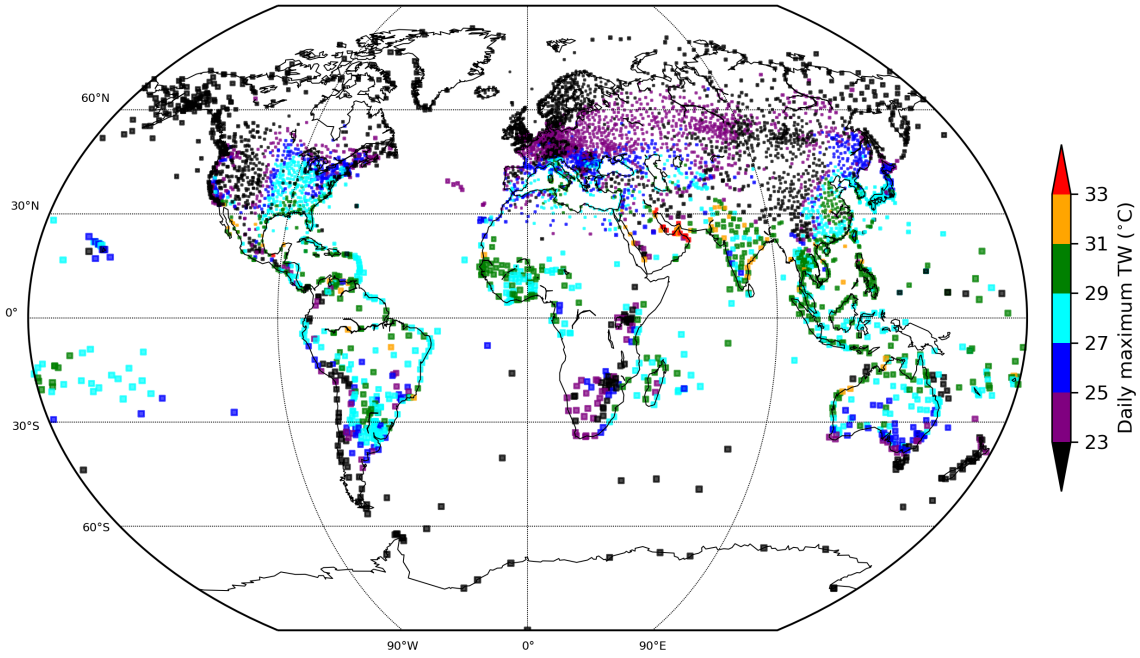

Fig. 1. Observed global extreme humid heat. Color symbols represent the 99.9th percentile of observed daily-maximum TW for 1979-2017, for HadISD stations with at least 90% data availability over this period. Note that marker size is inversely proportional to station density.

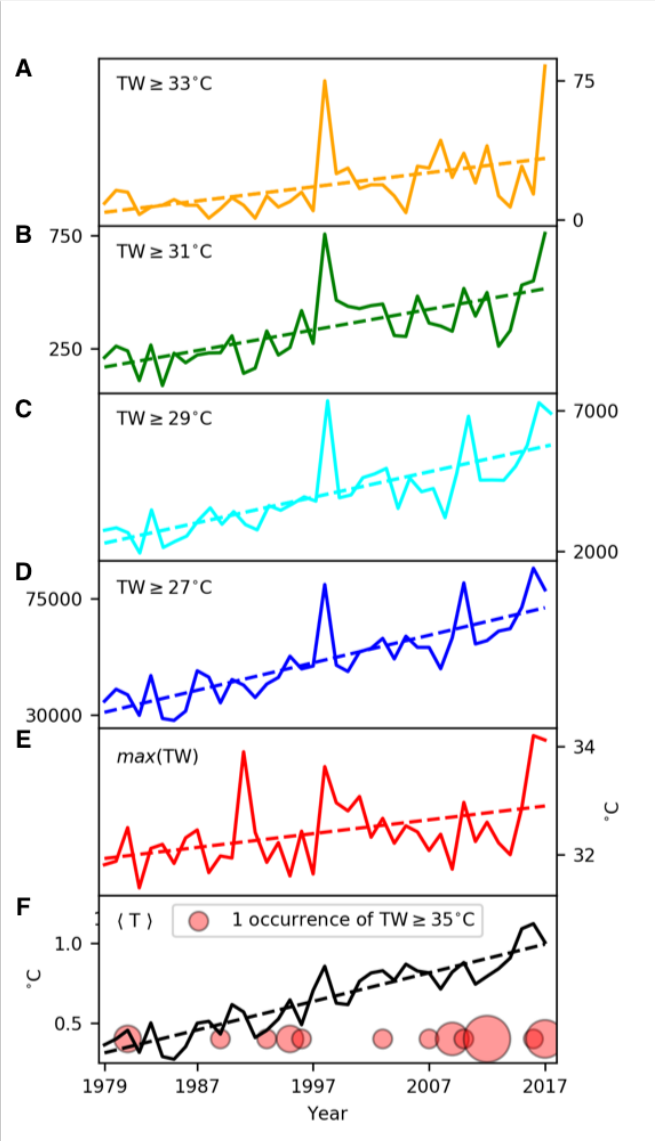

Fig. 2. Global trends in observed extreme TW. (A-D) Counts of TW exceedance (units are total annual station-days) above the thresholds labeled on the respective panel. We consider only stations with at least 90% data availability over 1979-2017. (E) Annual global maximum TW in the ERA-Interim reanalysis *(18)*. (F) The line plot shows global mean annual temperature anomalies (relative to 1850-1879) according to HadCRUT4 *(27)*; circles mark the rare station occurrences of TW exceeding 35°C, with radius linearly proportional to frequency.

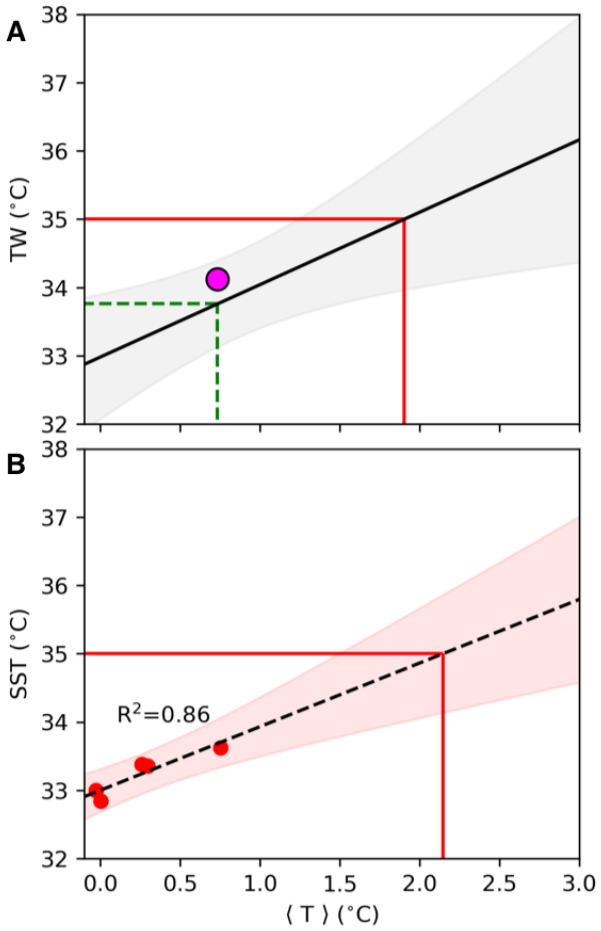

Fig. 3. Projections of most-probable global-mean warming associated with recurring exceedances of 35°C for global-maximum TW and SST. (A) Black line and gray shading show 30-year return periods of global-maximum TW predicted by the GEV model for the values of global warming since pre-industrial shown on the abscissa. Magenta circle is the empirical return period for the last 30 years (0.73°C); the dotted green line provides the corresponding GEV-based estimate. Red line denotes the amount of warming at which the GEV model predicts a maximum TW of 35°C. (B) Global-mean temperature anomaly over climate-normal periods and corresponding global-mean maximum SST. The fitted regression function is dotted, with goodness of fit annotated. The 95% prediction interval is enclosed within the shaded region, and the central estimate for when mean maximum SST rises above 35°C is denoted by the red lines.